

Inversion of superior mirage data to compute temperature profiles

Waldemar H. Lehn

Department of Electrical Engineering, University of Manitoba, Winnipeg, Manitoba R3T 2N2, Canada

Received May 5, 1983

Information derived from the superior mirage is used to compute the average vertical temperature profile in the atmosphere between the observer and a known object. The image is described by a plot of ray-elevation angle at the eye against elevation at which that ray intersects the object. The computational algorithm, based on the tracing of rays that have at most one vertex, iteratively adjusts the temperature profile until the observed image characteristics are reproduced. An example based on an observation made on the Beaufort Sea illustrates the process.

INTRODUCTION

The superior mirage is seen under conditions of temperature inversion. A mirage observation can be considered completely described by three basic elements: (1) an object at a known distance from the observer, (2) the transmitted image of this object, and (3) the average vertical temperature profiles in the atmosphere between the observer and the object. In principle, if any two of these elements are known, it should be possible to deduce the third. Thus, depending on which element is the unknown, we can formulate three distinct problems.

The most straightforward problem is the case in which elements (1) and (3) are known and the transmitted image is sought.¹⁻⁵ Of the two remaining inverse problems, the one examined here will attempt to extract the temperature profile from knowledge of elements (1) and (2).

Recent work on the inversion of refraction data has been carried out by Fleagle,⁶ Fraser,⁷ Mach,⁸ and others. Mach and Fraser⁹ also outline some of the previous methodology, listing a number of references.

The method of this paper, applied to the superior mirage, uses an iterative computational approach based on ray tracing for a single object at a fixed distance.

ASSUMPTIONS

The atmosphere is modeled as a set of fixed spherical shells concentric with the Earth. The smallest of these shells is taken to represent the Earth's surface, typically water or sea ice. The temperature distribution is specified by values at the layer boundaries, and between these points the temperature profile is taken to be linear. The ray path within each layer is well represented by a parabolic arc.^{1,10}

It is assumed that the paths of all light rays contributing to the observed image contain at most one maximum (vertex). This assumption limits applications to the frequently observed short- and medium-range cases that display at most one inverted image.¹¹

The nature of the image observed from a known object plane is completely specified by a single curve, termed a transfer characteristic (TC). The TC is a map of ray-eleva-

tion angle ϕ at the eye, plotted against the elevation z at which this ray intersects the object plane. Zero references for ϕ and z are, respectively, the local horizontal as defined by a level bubble and the (smooth) Earth's surface. For a standard atmosphere,¹² the TC is essentially a straight line, whose positive slope decreases with increasing object distance.

In the presence of strong temperature inversions, the TC can become a complex curve, with multiple ϕ values corresponding to a single z value. With the one-vertex restriction on light rays, the TC typically has one maximum and one minimum z , of the form shown in Fig. 1. The negative-slope portion describes the inverted image.

COMPUTATIONAL ALGORITHM

By varying the vertical temperature distribution, the computation seeks to reproduce a TC that has been derived from a field observation. A cybernetics process widely used in engineering is applied here: A problem that is relatively easy to solve, such as TC generation from a known temperature profile, is placed in the feedback path, with the result that the whole system in the forward direction solves the inverse problem of temperature-profile generation from the TC (see Fig. 2).

The critical points on the S-shaped TC are the values of maximum and minimum z . The maximum is called the pivot, with coordinates ϕ_p and z_p ; the minimum has coordinates ϕ_m and z_m . These points provide the basis for dividing the TC into three zones (Fig. 3), for each of which specific assumptions are made and distinct calculation procedures employed.

Zone I, further discussed in Appendix A, is the region below the pivot: $\phi_h \leq \phi < \phi_p$, where ϕ_h is the elevation of the horizon. Rays in this zone generate the lowest, erect part of the image. Although they possibly are curved, these rays are assumed to possess no vertices between observer and object plane. A necessary condition for no vertices is that $\phi_h \leq 0$. Also, for good convergence, the pivot angle ϕ_p should be a few arc minutes above the horizontal.

The calculations in zone I are based on the relation between the temperature gradient and the radius of curvature of a light ray. The process is not iterative; the calculations are carried

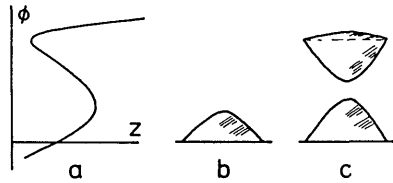


Fig. 1. a, A common TC that transforms b, an object, into c, two erect and one inverted image.

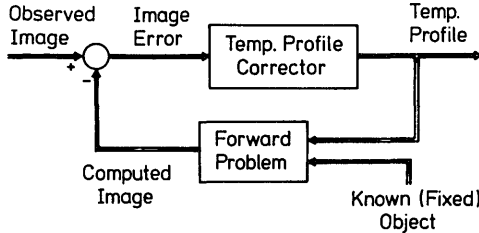


Fig. 2. The process of inversion.

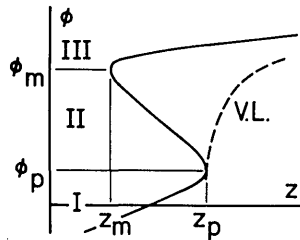


Fig. 3. Transfer characteristic zones (I, II, III) and a typical vertex locus.

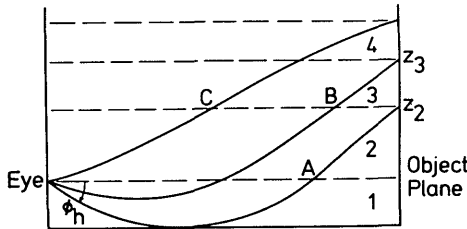


Fig. 4. The layers below the pivot. The spherical layer boundaries are represented as straight lines.

out once and produce a good fit to the TC for $\phi < \phi_p$ and hence a good estimate of the temperature profile for $z < z_p$.

The calculation sequence can be followed with the aid of Fig. 4. A radius of curvature is identified for each layer; then, knowing the eye-level temperature, we can find the temperatures at the remaining layer boundaries. Beginning with layer 1, below eye level, we find the radius necessary to match the observed horizon elevation ϕ_h corresponding to a ray tangent to the ground. Further projection of this ray generally leads to emergence from layer 1 at A, after which the ray must continue in layer 2. The unknown radius in layer 2 is adjusted so that the ray meets the object plane at its known final elevation z_2 . The remaining rays, for which $\phi < \phi_p$, are now projected out until they emerge from the known layer 2 at B and C. The layer 3 radius is identified by forcing the ray from B to reach its known destination z_3 , and the process is continued for all ϕ below the pivot ϕ_p . The governing equations, based on a parabolic representation of the rays, the layers, and the Earth's surface, can be found in Appendix A.

Zone II is the region responsible for the inverted image. It encompasses eye angles in the range $\phi_p \leq \phi \leq \phi_m$. The lim-

iting ray that forms the transition between zones I and II is the ray that has a vertex right at the object plane; it defines the pivot. The rays of zone II possess a caustic, which is nearly the locus of the ray vertices; and the pivot is the intersection of the caustic with the object plane.

The simple radius algorithm is not effective in zone II since the rays in this zone reach the object plane after returning from a higher elevation. An attempt to iterate the temperature profile on the basis of a correction at the object plane elevation would also fail because it would not influence the temperature in the vertex region. However, an algorithm can be constructed from the relation that exists among the vertex elevation, vertex temperature, and ϕ . At a vertex the following equation applies¹:

$$2\epsilon[\rho(z) - \rho(z_e)] + \frac{2}{R_E}(z - z_e) + \phi^2 = 0, \quad (1)$$

where

ρ is the density of the air,

R_E is the radius of the Earth,

z_e is the elevation of the observer's eye, and

$\epsilon = 0.000226$, from the refractive index of air $n = 1 + \epsilon\rho$.

Since density is a function of temperature, Eq. (1) can be rearranged into an expression for the vertex temperature T_v as a function of ϕ and vertex elevation z_v :

$$T_v - T(z_e) = T(z_e) \left[-\frac{g\beta}{T_m}(z_v - z_e) + \frac{T(z_e)(z_v - z_e)}{\epsilon\beta\rho_0 R_E} + \frac{T(z_e)\phi^2}{2\epsilon\beta\rho_0} \right]. \quad (2)$$

See Appendix B for details.

To begin the iteration within zone II, an initial guess—usually a linear increase with elevation—is made for the temperature profile above the pivot. The TC corresponding to the current estimate of the temperature profile is calculated. For each ray the vertex elevation is also recorded, making it possible to plot a locus of these vertices on the z, ϕ plane; see Fig. 3. The difference between the estimated and given TC is then used to adjust the slope of the vertex locus. Starting at the pivot, where the vertex locus is by definition tangent to the TC, these slopes are used to find a new set of vertex elevations. These, together with the corresponding ϕ values, permit calculation of new vertex temperatures by means of Eq. (2); and the set of new vertex elevations and temperatures constitutes the temperature profile for the next iteration.

For example, if a ray is too high on the object plane (estimated TC elevation exceeds given TC elevation), then the vertex locus will be steepened ($d\phi/dz$ increased), lowering the vertex of this ray and thus lowering its intersection with the object plane. In this way a TC error at any level is translated into a correction at the vertex level.

Zone III makes up the uppermost part of the observed image. The lowest few rays will have vertices, but most do not. They generate an elevated erect image, usually compressed. These rays have basically penetrated the inversion and for higher ϕ escape into space.

The computational approach used in zone III is relatively unrefined: absence of vertices is assumed, and the error in the TC (for each ϕ) is used to adjust the gradient of the tem-

perature profile. If the estimated elevation at the object plane is too high, the temperature gradient dT/dz is increased at the appropriate elevation in order to refract the ray downward. Conversely, if the estimate is too low, dT/dz is decreased.

EXAMPLE

The procedure was tested on several atmospheres, for which the TC had been calculated previously from a known temperature profile. In each case the algorithm converged rapidly, producing a reasonable approximation to the temperature profile in three iterations and a good approximation in eight iterations.

As an example, consider the photograph of Fig. 5a. It shows an 18.7-m hill, Whitefish Summit, photographed over sea ice from a distance of 20 km at Tuktoyaktuk, Northwest Territories, Canada. A superior mirage of this hill is shown to the same scale in Fig. 5b. Measurement of corresponding points on the photographs gives the observed TC; see Fig. 6a.

Two of the computer-produced temperature profiles, for iterations 3 and 8, are shown in Fig. 7. A fixed reference point on these curves is the known temperature of -2°C at eye level, 2.5 m above the ice. The corresponding TC's are shown in Fig. 6, in which it can be seen that iteration 8 produces a very good

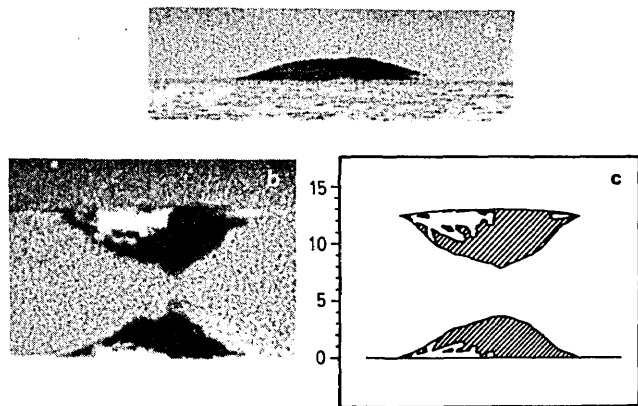


Fig. 5. a, Normal view of Whitefish Summit, May 20, 1979, 19.36 h MDT; b, superior mirage of Whitefish Summit, May 16, 1979, 03.22 h MDT; and c, calculated image based on the iteratively estimated temperature profile. The angular scale (in arc minutes) is the same for all figures.

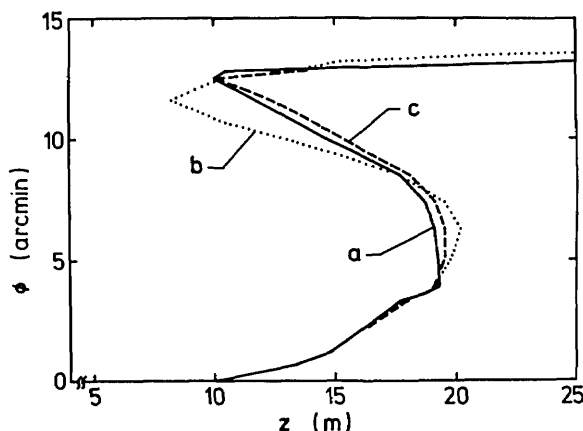


Fig. 6. Transfer characteristics: a, observed; b, calculated in iteration three; c, calculated in iteration eight and used to create Fig. 5c.

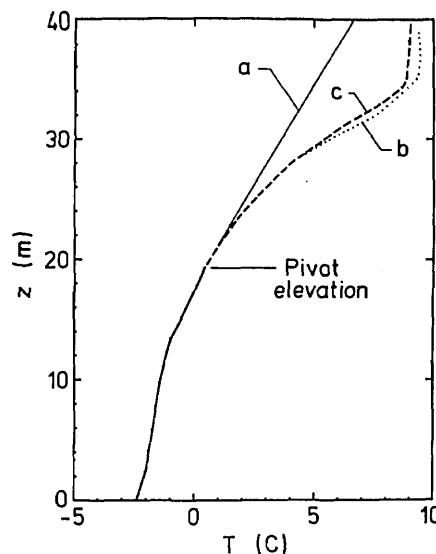


Fig. 7. Temperature profiles: a, initial guess; b, iteration 3; c, iteration 8, the final approximation. The portion below the pivot, corresponding to zone I, is calculated only once.

estimate of the original TC. The drawing of the distorted summit, Fig. 5c, is prepared from this last iteration. The calculated image agrees closely with the photographed observation.

The good agreement between the observation and the computer reconstructions indicates that the algorithm proposed here is a valid method for short- and medium-range inversion problems and that Fig. 7 is a reasonable estimate of the average temperature profile.

The basic nature of this profile is similar to one deduced from solar observations earlier during the same night.¹³ The temperature gradient is fairly low near the surface and increases with elevation. Such a profile supports optical ducting, which was indeed present at the time.

APPENDIX A

In zone I, the temperature gradient is deduced from the radius of curvature of the light rays by means of the relation¹⁴

$$\frac{1}{r} = \frac{\epsilon\rho}{(1 + \epsilon\rho)T} \left(\frac{dT}{dz} + g\beta \right), \tag{A1}$$

where g is the acceleration of gravity and $\beta = 0.00348$ mks units (the reciprocal of the specific gas constant R_M). In Eq. (A1), which holds for roughly horizontal rays, a positive value of r indicates refraction toward the Earth.

Because the radii are large, all circular arcs in the computation are represented as small portions of parabolas. Thus, in a rectangular coordinate system in which the x axis is tangent to the Earth and the z axis points vertically up, the Earth's surface is accurately approximated by

$$z = -\frac{x^2}{2R_E}, \tag{A2}$$

where R_E is the Earth's radius. Similarly, a concentric layer of height h above the surface would have the equation

$$z = -\frac{x^2}{2R_E} + h. \tag{A3}$$

An arc of ray is also represented in this way:

$$z = -\frac{x^2}{2r} + x \tan \phi + z_e, \quad (\text{A4})$$

where z_e is the elevation of the ray above the Earth's surface at the observer's eye, ϕ is the ray-elevation angle at its starting point, as previously defined, and r is the radius of curvature of the ray.

The elevation of the horizon ϕ_h is produced by the ray that is tangent to the Earth's surface. At the point of tangency, both the elevations and the slopes calculated from Eqs. (A2) and (A4) are equal. The two resulting simultaneous equations can be solved for the radius of ray curvature between eye level and the surface and the distance x_h to the point of tangency:

$$r = \left(\frac{1}{R_E} - \frac{\tan^2 \phi_h}{2z_e} \right)^{-1} \quad (\text{A5})$$

and

$$x_h = \left(\frac{1}{r} - \frac{1}{R_E} \right)^{-1} \tan \phi_h. \quad (\text{A6})$$

At a distance of $2x_h$, this ray again has elevation z_e and leaves this layer. Because this bottom layer, between eye and surface, is generally thin and contains few light rays, no more attention will be given it.

One more relation is required to carry out the computations for projecting a ray. The point at which a ray enters a new layer becomes the origin for the next ray projection. The elevation angle ϕ' with which the ray leaves the new origin is equal to the difference between the slope angles of the ray and the layer boundary. With the approximation $\tan \phi = \phi$, the equation is

$$\phi' = \frac{x}{R_E} - \frac{x}{r} + \phi. \quad (\text{A7})$$

A few special cases should be mentioned. If the object plane is sufficiently close, the intersection of this plane with the Earth's surface will be visible. In this case the lowest ray of interest, with elevation ϕ_b , passes directly to the base of the object, without becoming tangent to the surface. Then the calculations for ϕ_h are not relevant. Further, if ϕ_h or ϕ_b is positive, these rays must possess vertices in order to reach their destinations. In this case zone I does not exist, and calculations begins with zone II. Finally, a low pivot ($\phi_p \leq 0$) is indicative of an over-long horizontal range, beyond that which the algorithm can handle.

APPENDIX B

Atmospheric density can be expressed in terms of pressure p and absolute temperature T^{14} :

$$\rho = \beta p / T. \quad (\text{B1})$$

If the vertical temperature profile $T(z)$ is known, the pressure can be replaced by^{3,4}

$$p(z) = p_0 \exp \left[-g\beta \int_0^z \frac{dz'}{T(z')} \right], \quad (\text{B2})$$

where p_0 is the surface atmospheric pressure.

For the bottom 50 m of the atmosphere, the exponent is small, and the exponential is nearly unity. Little accuracy

is lost if we replace $T(z')$ by a constant value T_m , the estimated mean temperature in the layers of interest. The exponential is next approximated by the first two terms in its power series, and Eq. (B2) becomes

$$p(z) = p_0 \left(1 - \frac{g\beta z}{T_m} \right). \quad (\text{B3})$$

For $z = 50$ m and $T_m = 273$ K, the numerical values in Eq. (B3) are

$$p(50) = p_0(1 - 0.00625), \quad (\text{B4})$$

where the term in parentheses accurately represents $\exp(-0.00625)$.

The equation for density is thus

$$\rho(z) = \frac{\beta p_0}{T(z)} \left(1 - \frac{g\beta z}{T_m} \right), \quad (\text{B5})$$

which is substituted into Eq. (1) and solved for the vertex temperature $T_v = T(z_v)$. When higher-order terms are neglected, the result is Eq. (2), as previously given.

ACKNOWLEDGMENTS

This research received support from the Alexander von Humboldt Foundation, Germany, the Natural Sciences and Engineering Research Council, Canada, the Department of Indian and Northern Affairs, Canada, the Polar Continental Shelf Project, Canada, and the Research Board of the University of Manitoba, Canada.

REFERENCES

1. J. M. Pernter and F. Exner, *Meteorologische Optik*, 2nd ed. (Braumüller, Vienna, 1922).
2. A. B. Fraser, "Solutions of the refraction and extinction integrals for use in inversions and image formation," *Appl. Opt.* **16**, 160-165 (1977).
3. W. H. Lehn and H. L. Sawatzky, "Image transmission under arctic mirage conditions," *Polarforschung* **45**, 120-128 (1975).
4. W. H. Lehn and M. B. El-Arini, "Computer-graphics analysis of atmospheric refraction," *Appl. Opt.* **17**, 3146-3151 (1978).
5. An extensive list of references to research before 1935 can be found in W. -E. Schiele, "Zur Theorie der Luftspiegelungen," *Veroeff. Geophys. Inst. Univ. Leipzig* **7**, 103-188 (1935).
6. R. G. Fleagle, "The temperature distribution near a cold surface," *J. Meteorol.* **13**, 160-165 (1956).
7. A. B. Fraser, "Simple solution for obtaining a temperature profile from the inferior mirage," *Appl. Opt.* **18**, 1724-1731 (1979).
8. W. H. Mach, "Measurement of micrometeorological temperature profiles by the inversion of optical data," Ph.D. Thesis (Pennsylvania State University, University Park, Pa., 1978).
9. W. H. Mach and A. B. Fraser, "Inversion of optical data to obtain a micrometeorological temperature profile," *Appl. Opt.* **18**, 1715-1723 (1979).
10. R. Meyer, "Die Entstehung optischer Bilder durch Brechung und Spiegelung in der Atmosphäre," *Meteorol. Z.* **52**, 405-408 (1935).
11. In this context the concept of range is not absolute; it is linked to the nature of the image. Images of the requisite type may occur at object distances over 20 km, if the inversion has its steepest gradient 30 m above the observer's eye, or at 1 km for inversions less than 1 m above the observer.
12. The U.S. Standard Atmosphere is tabulated in Ref. 14. In the boundary layer, this atmosphere has a temperature gradient of -6.5 K/km.
13. W. H. Lehn and B. A. German, "Novaya zemlya effect: analysis of an observation," *Appl. Opt.* **20**, 2043-2047 (1981).
14. R. G. Fleagle and J. A. Businger, *An Introduction to Atmospheric Physics*, 2nd ed. (Academic, New York, 1980).